

1 **Selection of hydrological signatures for large-sample hydrology**

2  
3 N. Addor<sup>1,2\*</sup>, G. Nearing<sup>3</sup>, C. Prieto<sup>4</sup>, A. J. Newman<sup>1</sup>, N. Le Vine<sup>5</sup>, M. P. Clark<sup>1</sup>

4  
5 <sup>1</sup>Hydrometeorological Applications Program, Research Applications Laboratory,  
6 National Center for Atmospheric Research, Boulder, USA

7 <sup>2</sup>Climatic Research Unit, School of Environmental Sciences, University of East Anglia,  
8 Norwich, UK

9 <sup>3</sup>University of Alabama, Tuscaloosa, USA

10 <sup>4</sup>Environmental Hydraulics Institute “IHCantabria”, University of Cantabria, Santander,  
11 Spain

12 <sup>5</sup>Department of Civil and Environmental Engineering, Imperial College, London, UK

13 \*Corresponding author: N.Addor@uea.ac.uk

14  
15 **Key points**

16  
17 There is a need for a framework to support the selection of hydrological signatures for  
18 experimental and modeling studies.

19 We rank signatures based on their predictability in space, different predictions methods  
20 yielding very similar results.

21 We identify difficulties emerging when moving down the ranking, which can  
22 compromise the utility and reliability of the signatures.

23  
24 **Abstract**

25  
26 Hydrological signatures are now used for a wide range of purposes, including catchment  
27 classification, process exploration and hydrological model calibration. The recent boost  
28 in the popularity and number of signatures has however not been accompanied by the  
29 development of clear guidance on signature selection, meaning that signature selection is  
30 often arbitrary. Here we use three complementary approaches to compare and rank 15  
31 commonly-used signatures, which we evaluate in 671 US catchments from the CAMELS  
32 data set (Catchment Attributes and MEteorology for Large-sample Studies). Firstly, we  
33 employ machine learning (random forests) to explore how attributes characterizing the  
34 climatic conditions, topography, land cover, soil and geology influence (or not) the  
35 signatures. Secondly, we use a conceptual hydrological model (Sacramento) to critically  
36 assess which signatures are well captured by the simulations. Thirdly, we take advantage  
37 of the large sample of CAMELS catchments to characterize the spatial smoothness (using  
38 Moran’s  $I$ ) of the signature field. These three approaches lead to remarkably similar  
39 rankings of the signatures. We show that signatures with the noisiest spatial pattern tend  
40 to be poorly captured by hydrological simulations, that their relationship to catchments  
41 attributes are elusive (in particular they are not correlated to climatic indices like aridity)  
42 and that they are particularly sensitive to discharge uncertainties. We question the utility  
43 and reliability of those signatures in experimental and modeling hydrological studies, and

44 we underscore the general importance of accounting for uncertainties in hydrological  
45 signatures.

## 46 **1 Introduction**

47  
48 Hydrological signatures (indices characterizing hydrologic behavior) are now commonly  
49 used to understand space-time variability in hydrological processes (Troch et al., 2009;  
50 Sawicz et al., 2011) and to diagnose weaknesses in hydrological models (Gupta et al.,  
51 2008; Euser et al., 2013; Vrugt and Sadegh, 2013). Signatures can be computed using a  
52 wide range of data sources (such as soil moisture or snow data), but in practice they are  
53 most often computed using discharge time series (e.g., Yilmaz et al., 2008). Hydrological  
54 signatures are particularly useful to characterize and compare the dynamics of large  
55 samples of catchments, for which only limited observations are available (discharge is  
56 measured, but evapotranspiration, snow water equivalent, tracer concentrations or water  
57 table level are usually not measured). In a sense, hydrological signatures are an indirect  
58 way to explore hydrological processes, when those processes cannot be isolated because  
59 of the lack of measured data. This enables in particular catchment classification (Sawicz  
60 et al., 2011) and provides insights into hydrological behavior in places where little to no  
61 data are available (Kuentz et al., 2017).

62  
63 A profusion of hydrological signatures already exists, and more are being developed. The  
64 diversity of hydrologic signatures enables characterizing a wide variety of hydrological  
65 features, but at the same time, makes selecting appropriate signatures challenging  
66 (McMillan et al., 2017). There are some general selection criteria; for instance, it is  
67 desirable that i) signatures can be related to hydrological processes to enable a better  
68 understanding of particular aspects of catchment behavior, ii) they are sensitive to  
69 processes occurring over different periods (from the sub-daily to the decadal time scale),  
70 and iii) they are not redundant. Yet, signature selection is essentially dealt with on a case-  
71 by-case basis, different studies invariably use different signatures, and the same  
72 signatures may be computed in different ways (e.g., the baseflow index). While it is  
73 normal that each study selects signatures to meet its specific needs, there is a need to  
74 develop general guidance on the selection of hydrologic signatures.

75  
76 Our key contribution is a general framework to understand the utility of different  
77 signatures. Previous work has focused on specific aspects of signatures like their  
78 regionalization (Beck et al., 2015; Almeida et al., 2016), their sensitivity to discharge  
79 measurement errors (Westerberg et al., 2016) or their use for model calibration (Euser et  
80 al., 2013; Hrachowitz et al., 2014) or model selection (Clark et al., 2011; McMillan et al.,  
81 2011). All these aspects are important for signature selection, but they are difficult to  
82 account for simultaneously. Although the studies just mentioned are related, they have  
83 been essentially conducted independently. This study aims to synthesize insights gained  
84 from different perspectives on hydrological signatures. We developed a framework to  
85 compare and organize 15 commonly-used signatures, which we evaluated over 671  
86 catchments in the contiguous United States (CONUS). We explore i) how well signatures  
87 can be predicted from catchments attributes (using random forests), ii) how well they can  
88 be simulated (using a conceptual hydrological model) and iii) how smoothly they vary in

89 space.

90

91 Our approach is motivated by the general idea that "the ability to accurately predict  
92 behavior is a severe test of the adequacy of knowledge in any subject" put forward by  
93 Crawford and Linsley (1966). We argue that the failure to predict a signature is  
94 symptomatic of limitations of our understanding of what it represents, and/or of  
95 limitations of data we use to compute or predict it. Here we explore and reveal limitations  
96 of hydrological signatures, and argue that this can help to guide signature selection. Our  
97 approach is driven by three main research questions:

98

- 99 1. How well can signatures be predicted using landscape characteristics? With this  
100 question, we try to better understand how the interplay of landscape attribute shape  
101 hydrological behavior. We used a statistical model (random forests) to relate  
102 catchments attributes to hydrological signatures.
- 103 2. How well can signatures be simulated by a conceptual hydrological model calibrated  
104 using an aggregated measure of performance? We used signatures to critically assess  
105 the realism of simulations from a model calibrated using RMSE. Our aim is to  
106 examine shortcomings of simulations resulting from this kind of traditional (and still  
107 prevalent) parameter estimation technique.
- 108 3. How smoothly do signatures vary in space? We explored the spatial patterns of  
109 signatures drawn when plotting their value for 671 catchments. We used those  
110 patterns to reflect on whether signature variations in space truly reflect differences in  
111 hydrological processes, or rather, data and method uncertainties.

112

113 The analysis in this paper enables us to compare and rank signatures, and to provide  
114 general guidance for their selection and use. The remainder of this paper is organized as  
115 follows: The data and methods are presented in Section 2; the ranking of signatures is  
116 presented in Section 3; the implications for signature selection are discussed in Section 4;  
117 conclusions and future research needs are presented in Section 5.

## 118 **2 Data and methods**

### 119 **2.1 The CAMELS data set**

120 All the data used in this study come from the CAMELS data set (Catchment Attributes  
121 and MEteorology for Large-sample Studies). The CAMELS data set covers 671  
122 catchments in the contiguous US (CONUS) and consists of two types of data: daily time  
123 series the atmospheric forcing and discharge (Newman et al., 2014, 2015) and catchment  
124 attributes selected to provide a quantitative description of landscape features likely to  
125 influence hydrological processes (Addor et al., 2017a, 2017b). The hydrometeorological  
126 time series and catchment attributes are described in Sections 2.2 and 2.3, respectively.

### 127 **2.2 CAMELS hydrometeorological time series**

128 The hydrometeorological time series include both daily meteorological forcing and  
129 observed discharge time series, as well as daily hydrological simulations. Precipitation  
130 and temperature at the catchment scale were retrieved from the Daymet data set

131 (Thornton et al., 2012). Potential evapotranspiration was estimated based on Priestley and  
132 Taylor (1972). The hydrologic simulations were produced using the Sacramento Soil  
133 Moisture Accounting model (Burnash et al., 1973) combined with the SNOW-17 snow  
134 accumulation and ablation model (Anderson, 1973), with streamflow being routed using  
135 a unit-hydrograph model. Hereafter this modeling setup is referred to as SAC. SAC was  
136 calibrated using the shuffled complex evolution (SCE, Duan et al., 1992) global  
137 optimization routine, minimizing the root mean squared error (RMSE) of the discharge  
138 simulations. Simulations started on October 1<sup>st</sup> 1980 for the 598 basins (out of 671) for  
139 which discharge measurements started on or before that date. For the other basins,  
140 simulations started on the first October 1<sup>st</sup> after the start of the discharge records. SAC  
141 was calibrated over the first 15 years of the simulation for each catchment, meaning that  
142 different periods were used for different catchments. For each catchment, SCE was  
143 started from 10 different random seeds, which led to 10 optimized parameter sets. Further  
144 details on the hydrometeorological time series are provided in Newman et al. (2015).

### 145 **2.3 CAMELS catchment attributes**

146 The landscape of each catchment was described using a wide range of attributes, which  
147 can be divided into five classes:

148

- 149 1. Topographic characteristics: features such as catchment area and mean elevation,  
150 extracted from the United States Geological Survey (USGS) data base.
- 151 2. Climatic indices: indices such as aridity and the frequency of high precipitation  
152 events, computed using the Daymet (Thornton et al., 2012) daily time series  
153 extracted by Newman et al. (2015).
- 154 3. Land cover characteristics: attributes such as the maximum leaf area index and the  
155 rooting depth, estimated using MODIS imagery.
- 156 4. Soil characteristics: variables such as the soil depth and the sand fraction,  
157 extracted from the State Soil Geographic Database (STATSGO, Miller and White,  
158 1998) and from Pelletier et al. (2016).
- 159 5. Geological characteristics: characteristics such as the dominant geology class and  
160 the subsurface permeability, retrieved from Global Lithological Map (GLiM,  
161 Hartmann and Moosdorf, 2012) and GLobal HYdrogeology MaPS (GLHYMPS,  
162 Gleeson et al., 2014).

163

164 The complete list of catchment attributes, as well as details on the methods and data used  
165 to compute them, is provided in Table 1. Note that not all of the CAMELS attributes were  
166 used. We excluded the following attributes to avoid redundant information and clarify the  
167 result of the statistical analysis: the leaf area index difference and green vegetation  
168 fraction difference (both are highly correlated with the leaf area index maximum), mean  
169 slope (correlated with mean elevation, but more delicate to estimate), soil porosity and  
170 conductivity (both are highly correlated with the sand fraction because of their estimation  
171 relying on sand fraction) and the second dominant geological class of the GLiM data set  
172 (as it is unavailable for 138 catchments, which are entirely covered by a single class).

173

174 To characterize the hydrological behavior of the catchments, we computed 15

175 hydrological signatures. Those signatures were selected because they characterize  
176 different parts of the hydrograph and they are sensitive to processes occurring over  
177 different time scales. They are also commonly employed in the literature, so we used this  
178 study as an opportunity to compare them. The signatures we considered are described in  
179 Table 2. We computed them using the observed discharge and the mean of the 10 SAC  
180 simulations produced for each catchment. We also predicted these signatures based on  
181 catchment attributes using random forests (Section 2.4). We evaluated the signatures  
182 simulated by SAC and predicted by random forests by computing the fraction of variance  
183 ( $R^2$ ) of the observed signatures that they explain. The number of stations used for  $R^2$   
184 computation varies slightly from signature to signature, because in some specific  
185 situations, for instance when rivers are dry for significant periods, the signatures cannot  
186 be computed. The number of catchments for each signature is however always greater  
187 than 600.  $R^2$  is unitless, which enables the direct comparison of different signatures. All  
188 the signatures were computed using daily discharge data scaled by the catchment area.  
189 Further details on the data and methods used to compute the catchment attributes and  
190 hydrological signatures are provided in Addor et al. (2017b).

#### 191 **2.4 Random forests to predict hydrological signatures using catchment attributes**

192 We used random forests to predict hydrological signatures using catchment attributes.  
193 Random forests are a machine-learning algorithm relying on a large number of regression  
194 trees to produce an ensemble of predictions. They have been successfully used in a  
195 various fields of geosciences, for instance to predict hydrological signatures (Snelder et  
196 al., 2009) and soil characteristics (Chaney et al., 2016; Hengl et al., 2017). We provide a  
197 brief introduction to random forests in Appendix 1. For more detailed information, we  
198 refer the reader to Breiman (2001). We developed random forests in R (R Core Team,  
199 2017) using the package randomForest (Liaw and Wiener, 2002). For an introduction to  
200 random forests using R, we recommend James et al. (2013).

201

202 We selected random forests for the data mining of the CAMELS data set for the  
203 following reasons:

204

- 205 1. Random forests allow for multiple predictors and non-linear relationships: It is  
206 common to use a single characteristic (typically aridity or the baseflow index) to  
207 summarize hydrological behavior and differentiate between catchments. Yet,  
208 catchment behavior is never determined by a single attribute, but instead reflects the  
209 interplay of numerous attributes. Beck et al. (2015) explored streamflow  
210 characteristics for thousands of catchments and concluded that "the individual  
211 relationships between catchment attributes and Q characteristics were generally weak,  
212 suggesting the need for models incorporating multiple predictors to estimate Q  
213 characteristics". Random forests are well-adapted for this task because they allow for  
214 multiple predictors, and since they are constructed using a series of thresholds, they  
215 can outperform classical multiple linear regressions when the response is not linear.

216

- 217 2. Random forests are not limited by our understanding of catchment behavior: Random  
218 forests are a flexible statistical model, which is not constrained by any physical  
219 principles or assumptions on hydrological processes. We see it as an advantage, as  
220 data exploration using random forest can potentially reveal relationships, which are  
221 not commonly acknowledged, although they can be explained a posteriori from a  
222 physical perspective.  
223
- 224 3. Reduced risk of data overfitting: Random forests are an ensemble of regression trees,  
225 which gives them more robustness than individual regression trees. Randomness is  
226 introduced when they are constructed so that their predictions are not overly  
227 influenced by specific catchments or predictors (Appendix 1). The random forest  
228 predictions were evaluated using a ten-fold cross-validation: a random forest was  
229 trained using 90% of the basins and its predictions were evaluated using the  
230 remaining basins, this procedure was then repeated nine additional times in order to  
231 cover all the basins. The results showed hereafter are for the validation phase, not for  
232 the training phase.  
233
- 234 4. Transparency and interpretability: When producing multi-variable predictions, it is  
235 important to be able to assess which predictors have the greatest influence on the  
236 response variables. Interpreting the coefficients of a multiple regression is an option  
237 (e.g., Almeida et al., 2012), but this does not deliver as clear of a picture, because  
238 there can be differences between the predictors of several orders of magnitude. In  
239 contrast, the interpretation of the influence of each predictor in the random forest  
240 using IncMSE is straight-forward (IncMSE is the relative increase in the MSE of the  
241 prediction when the values of the predictor of interest are shuffled, see Appendix 1).  
242
- 243 5. Good performance in prediction mode and reliable uncertainty estimates: Random  
244 forests and similar machine-learning techniques (such as neural network, e.g. Beck et  
245 al., 2015) can deliver accurate predictions for little computation effort (growing each  
246 forest takes a few seconds). Further, each random forest relies on an ensemble of  
247 trees, that can be used to estimate the uncertainty of the prediction (those uncertainty  
248 estimates can be very reliable, see Figure A1d).  
249

250 We argue that these advantages justify the use of random forests in our study. It is  
251 however fair to acknowledge that random forests also have drawbacks. Critically, they  
252 are highly parameterized, as each regression tree uses on the order of 10 thresholds. In  
253 this study, we used 500 trees to predict each of the 15 hydrological signatures, which  
254 leads to about 70,000 parameters (thresholds on predictors). This number of parameter is  
255 impractical to analyze on an individual basis, but the relative influence of the predictors  
256 on each signature can be quantified using the IncMSE.

### 257 **3 Results**

258

259 The presentation of the results is organized as follows. We first present spatial maps for a  
260 subset of commonly used signatures (mean discharge, slope of the flow duration curve,  
261 and the baseflow index), and then we present statistics for the full set of 15 signatures.

262 Finally, we show the influence of individual catchment attributes on random forest  
263 predictions of different signatures.

### 264 **3.1 Simulation, prediction and spatial smoothness of hydrological signatures -** 265 **introduction**

266 Figure 1 illustrates predictions of three example hydrologic signatures (mean annual  
267 discharge, slope of the flow duration curve, and the baseflow index) from both random  
268 forests and the SAC model. Mean discharge can be predicted very well by a random  
269 forest based on catchment descriptors ( $R^2 = 0.92$ ) and can be also simulated remarkably  
270 well by the conceptual hydrological model SAC calibrated by minimizing the RSME ( $R^2$   
271  $= 0.98$ ). In contrast, the performance of both the random forest and SAC is poor when it  
272 comes to the slope of the flow duration curve ( $R^2 = 0.29$  and  $R^2 = 0.15$ , respectively). The  
273 baseflow index is predicted (by the random forest) and simulated (by SAC) better than  
274 the slope of the flow duration curve, but worse than the mean annual discharge ( $R^2 = 0.64$   
275 and  $R^2 = 0.84$ , respectively). Note that for these three signatures, the performance of the  
276 random forest and of SAC are related: both methods perform well for the mean annual  
277 discharge, reasonably well for the baseflow index, and poorly for the slope of the flow  
278 duration curve.

279  
280 Interestingly, the performance of both the random forest and SAC is related to the spatial  
281 smoothness of the hydrological signatures. Note how the mean discharge field varies  
282 smoothly across space, whereas the slope of the flow duration curve exhibits large  
283 changes over short distances (first row of Figure 1). To quantify the spatial smoothness,  
284 we used Moran's  $I$  to measure the spatial auto-correlation (Appendix 2).  $I$  enables us to  
285 quantify features that are clear visually, and to compare signatures based on the spatial  
286 smoothness of their field. The spatial smoothness is the highest for the mean discharge ( $I$   
287  $= 0.51$ ), intermediate for the baseflow index ( $I = 0.16$ ) and the lowest for the slope of the  
288 flow duration curve ( $I = 0.09$ ). This ranking is the same as the ranking based on the  
289 performance of the random forest and SAC. In other words, Figure 1 suggests that  
290 signatures with lower spatial smoothness may be harder to relate to catchment  
291 characteristics and to simulate using a conceptual model.

### 292 **3.2 Simulation, prediction and spatial smoothness of hydrological signatures -** 293 **evaluation for 15 signatures**

294 Figure 2 shows that there is a strong three-way relationship between how well signatures  
295 can be predicted based on catchment attributes, how well they can be simulated by SAC,  
296 and the smoothness of their spatial variability over the CONUS. The signatures in Figure  
297 2 are ordered from left to right based on how well they can be predicted using a random  
298 forest. Like for Figure 1, we compared the observed and predicted signatures from the  
299 random forest by computing the coefficient of determination  $R^2$ , shown in light blue in  
300 Figure 2.  $R^2$  varies from 0.92 (mean annual discharge) to 0.29 (slope of the flow duration  
301 curve). The performance of the random forest is compared to that of SAC, shown in dark  
302 blue in Figure 2. It is clear that hydrological signatures that can be accurately predicted  
303 from catchment attributes by the random forest can also be well simulated by SAC.  
304 Indeed, the performance of the random forest and that of SAC, each described by 15  $R^2$

305 values, are highly correlated ( $\rho = 0.91$ ). Note that several signatures we considered were  
306 also predicted by Beck et al. (2015) using characteristics from thousands of catchments  
307 from across the world and neural networks. They also find that some signatures are better  
308 predicted than others and interestingly, it appears that if they had ranked signatures based  
309 on the  $R^2$  they report in their Figure 5, the ranking would have been very similar to what  
310 we propose (with the mean annual flow and half-flow date being best predicted, followed  
311 by the high-flow quantile, and finally the low flow quantile and the baseflow index).

312  
313 Furthermore, the spatial smoothness measured by Moran's  $I$  (shown in green in Figure 2)  
314 is almost systematically greater for signatures that can be accurately predicted by the  
315 random forest and well simulated by SAC. In fact, the correlation between the  
316 performance of the random forest and spatial smoothness is strong ( $\rho = 0.91$ ). This  
317 suggests that random forests fail to capture sudden (small-scale) changes in hydrological  
318 signatures over short distances. The spatial smoothness also appears to be a good  
319 predictor of how well hydrological signatures are captured by SAC ( $\rho = 0.78$ ).

320  
321 The remarkable similarity between the performance of the random forests and SAC is  
322 somewhat surprising given that the two methods are fundamentally different. The random  
323 forest is based on catchment attributes (not on hydrometeorological time series, although  
324 some catchment attributes are shaped by hydrometeorological conditions described by the  
325 time series) and is a statistical framework that is not constrained by physical processes. In  
326 contrast, SAC is a conceptual hydrological model conditioned by hypotheses on  
327 catchment behavior imbedded in its formulation, it requires daily time series (random  
328 forests only have access to climatic averages) and its parameters are determined by an  
329 automated discharge calibration procedure (they were not inferred from catchment  
330 attributes). Further, the random forests were trained to capture each hydrological  
331 signature independently, but SAC was only trained to optimize RMSE (note that this does  
332 not prevent SAC from providing better estimates of most signatures, as shown by Figure  
333 2).

### 334 **3.3 Climatic indices as strongest predictors of hydrological signatures**

335 Recall from Figures 1 and 2 that hydrological signatures well predicted by random forests  
336 tend to have a smooth pattern. This can be explained by the strength of the climate signal:  
337 climatic indices have a smooth pattern over the CONUS, and when they are highly  
338 correlated to signatures, those signatures inherit their smooth pattern. This is clear in  
339 Figure 3: the spatial patterns of climate indices shown in the first row (originally selected  
340 by Berghuijs et al., 2014) are similar to the signatures in the second row. The maps of  
341 mean annual discharge and the runoff ratio show very similar patterns to that of the  
342 aridity map, while the half-flow date principally reflects the precipitation seasonality and  
343 the fraction of precipitation falling as snow. In contrast, the maps in the bottom row of  
344 poorly predicted signatures show a noisier spatial pattern and lack a clear relationship to  
345 the climatic indices shown in the first row.

346  
347 To better understand why some signatures were better predicted than others, we explored  
348 which predictors were preferentially used by the random forest. To this end, we consider



349 the IncMSE, the increase in the MSE of the prediction when the value for each predictor  
350 were shuffled. IncMSE is indicated by the size of the dots in Figure 4. The color of the  
351 dots indicates the Spearman rank correlation coefficient between each attribute and  
352 signature. Most of the influential predictors in the random forest are climatic variables. If  
353 we restrict attention to the 14 pairs of catchment attributes-hydrological signatures with  
354 IncMSE > 20%, 11 of them involve a climatic variable (aridity alone accounts for 6  
355 pairs). In this respect, the climatic indices exert a stronger influence on hydrological  
356 signatures than the topographic, soil, land cover and geological attributes combined.

357

358 The large influence of climatic conditions on hydrological behavior is not new. Aridity is  
359 commonly regarded as the main driver of water partitioning at the land surface (Budyko,  
360 1974; Hrachowitz et al., 2013). The influence of climate on hydrological regimes is well  
361 acknowledged (Berghuijs et al., 2014), yet it is debated whether this influence is direct,  
362 via the water balance, or indirect, via the long-term influence of climate on the landscape  
363 (Harman and Troch, 2014). Importantly, climatic variables do not only drive current, but  
364 probably also trends induced by climate change (Rice et al., 2016). Overall, our results  
365 are consistent with those of Beck et al. (2015), who predicted a range of hydrological  
366 signatures using catchment attributes and reported that climate indices exerted the  
367 strongest influence, while predictors related to soils and geology were less important.

368

369 The importance of aridity is clear and its control over the water balance receives  
370 continuous attention, sustained by the high number of studies based on the Budyko  
371 framework (Padrón et al., 2017). Yet, Figure 4 shows that several hydrological variables,  
372 which reflect key aspects of hydrological dynamics, are poorly predicted by aridity alone,  
373 or even by a combination of climatic indices. For instance, random forests were unable to  
374 clearly relate climate indices to the precipitation-streamflow elasticity, the slope of the  
375 flow duration curve or the no-flow frequency. The variations in space of these signatures  
376 (bottom row of Figure 3) appear to be too complex to be captured by correlation  
377 coefficients, or by a more complex statistical model (random forest) or by a conceptual  
378 hydrological model (SAC). In other words, the number of hydrological signatures that  
379 can be well predicted based on climatic indices alone is limited.

### 380 **3.4 Weak influence of land cover, soil and geology on hydrological behavior?**

381 We found that climatic indices have by far the greatest influence on selected hydrological  
382 signatures, while the attributes characterizing the land cover, soil, geology and  
383 topography have a much weaker influence. The lack of dark colors in the corresponding  
384 columns of Figure 4 indicate that those attributes, when considered individually, are not  
385 strongly correlated to hydrological signatures. Even when those attributes are combined  
386 with other attributes using a random forest, their influence is generally insignificant, as  
387 shown by the lack of the large circles in the same columns. The relative strength of  
388 climatic variables when compared to other catchment attributes has the following  
389 implication. When a hydrological signature is strongly linked to one or several climate  
390 indices, it is well predicted, and conversely, weak links lead to poor predictions. Hence,  
391 climatic attributes strongly condition how well hydrological signatures can be predicted  
392 by the random forest. Some signatures like the slope of the flow duration curve are not

393 well constrained by climate variables, and the random forest is not able to extract relevant  
394 information from the predictors we are using.

395  
396 The lack of significance of land cover, soil and geology attributes shown in Figure 4 is  
397 consistent with the finding of Beck et al. (2015), as mentioned previously. Merz and  
398 Bloschl (2009) similarly showed that event runoff coefficients in 459 Austrian  
399 catchments were barely influenced by land cover, soil types, and geology, and were better  
400 explained by climate-related indices. In contrast, when exploring and classifying 116  
401 near-natural catchments in the UK, Chiverton et al. (2015) found that geology, the depth  
402 to gleyed layer in soils and the percentage of arable land were good discriminants.  
403 Likewise, Singh et al. (2014) found geology and land use do matter when choosing donor  
404 catchments, but their influence depend on the region.

405  
406 We find that land cover, soil and geology attributes are weak predictors, yet this does not  
407 mean that land cover, soil and geology do not influence hydrological processes. It rather  
408 tells us that their influence on hydrological signatures can be missed by standard  
409 catchment attributes, data sets and machine learning techniques, such as those used in this  
410 study, for the following reasons:

- 411 1. Spatial scale: the scale that which vegetation, soil, geological processes occur is  
412 often several orders of magnitude smaller than what our finest data sets or models  
413 can capture. Key properties are difficult to measure in the first place and also  
414 difficult to upscale in a way that preserves their influence on water dynamics. For  
415 instance, aggregate soil types likely do not represent the heterogeneity that  
416 governs matrix flow in watersheds and essential information is lost when  
417 computing catchment-scale averages. This stresses the importance of upscaling  
418 methods preserving landscape properties across scales (Samaniego et al., 2010;  
419 Rakovec et al., 2016).
- 420 2. Data quality and uncertainty: Data quality has been brought up to explain why  
421 soil and geological data are not good predictors of hydrological signatures (Beck  
422 et al., 2015). It is indeed likely that issues related to data collection (see  
423 discussion in Addor et al., 2017b) limit the predictive power of soil data. Further,  
424 note that landscape attributes considered here are all deterministic, but data sets  
425 like SoilGrids (Hengl et al., 2017) provide uncertainty estimates of soil  
426 characteristics, which may improve the predictions and make the influence of  
427 soils on water dynamics clearer.
- 428 3. Machine learning algorithm: Random forests may not have the agility to extract  
429 the full information available in the data sets we used as predictors. They fail in  
430 particular at capturing sudden changes in space, for instance the fields in Figure 1j  
431 are too smooth, but the basic equations constituting SAC lead to more spatial  
432 diversity (Figure 1k), although the accuracy is low in both cases.
- 433 4. Land cover, soil and geology are secondary predictors: they may play a  
434 significant role in differentiating catchment responses when climatic conditions  
435 are almost fixed. This assumption could be tested in future studies, by breaking  
436 down the sample of 671 catchments into sub-samples of catchments of similar  
437 climatic conditions and by repeating the analysis conducted here.

438

439 These results stress that further work is needed to clarify the relationships between  
440 landscape attributes and hydrological signatures that are not well explained by  
441 climatic indices. Soil, geology and vegetation processes play an essential role in the  
442 water cycle, yet we find difficult it to capture their influence on discharge at the  
443 catchment scale, despite the diversity of hydro-climatic regimes and catchment  
444 attributes that we covered. We expect that predictions of hydrological signatures will  
445 be improved by better measurements and better upscaling techniques of catchment  
446 attributes, as well as by additional attributes, but that the improvements for climate-  
447 driven signatures will be more modest, since the predictions are already good.

## 448 **4 Discussion**

449

450 In the Results section we discussed how, as we move down the table of signatures shown  
451 in Figure 4, the quality of the predictions and simulations, the spatial smoothness of the  
452 signature fields and the influence of climate vary in consistent ways. We summarized  
453 these results in the top part of Table 3. In this Discussion section, we discuss the  
454 implications of these results for hydrologic research. We focus on challenges that emerge  
455 as we move down the table of signatures in three contexts: i) the sensitivity to discharge  
456 uncertainty and implications for signature regionalization, ii) the relation to hydrological  
457 processes and iii) the use of signatures for model calibration and evaluation.

### 458 **4.1 Sensitivity to discharge uncertainty and implications for signature** 459 **regionalization**

460 In this study, we do not explicitly characterize errors in discharge time series resulting  
461 from rating curve uncertainties, nor how those uncertainties propagate into hydrological  
462 signatures. These aspects were however investigated by Westerberg et al. (2016) for 43  
463 UK catchments. They found that the impacts of rating curve uncertainties on hydrological  
464 signatures depend on the catchment of interest and on the type of signature. Some  
465 signatures, such as the mean discharge, are far less sensitive to rating curve uncertainty  
466 than others, such as the slope of the flow duration curve (as illustrated by their Figure 6).  
467 Similarly, low flow signatures are more sensitive to data errors than high flow signatures.  
468 They also regionalized signatures following a weighted-pooling-group approach, in  
469 which each signature was estimated using the weighted mean of its value in similar  
470 catchments (similarity was defined based on mean annual precipitation, the 90<sup>th</sup> percentile  
471 catchment elevation, the base-flow index and catchment area). Their regionalization  
472 performs better for high flows than for low flows, and better for the mean discharge than  
473 for the slope of the flow duration curve (their Figure 8). This is not only consistent with  
474 the sensitivity of the signatures to rating curve uncertainties that they determined, but also  
475 with the ranking of signatures we propose based on random forest regionalization.

476

477 Westerberg et al. (2016) underscored that uncertainty in discharge time series  
478 complicates and deteriorates the regionalization of hydrological signatures. Here we do  
479 not characterize discharge uncertainties. Instead, we approach the regionalization  
480 challenge from a different perspective. Using a greater number of catchments and  
481 Moran's *I* as a measure of spatial correlation, we show that the signatures identified by  
482 Westerberg et al. (2016) as sensitive to rating curve uncertainty tend to vary abruptly

483 over short distances (low Moran's  $I$ , toward the bottom of the signature table shown in  
484 Figure 4). Those signatures would be poorly regionalized when selecting the closest  
485 catchments as donors, since the value of the signature typically vary significantly among  
486 those catchments (for reasons that are currently unclear). In other words, the spatial  
487 interpolation of signatures is easier when their field varies in smooth (predictable)  
488 fashion. It is likely that the sudden variations over space for some signatures, which we  
489 argue make regionalization difficult, come in part from discharge uncertainties.

#### 490 **4.2 Relation to hydrological processes – questionable discriminative power of** 491 **hydrological signatures**

492 An essential question, when it comes to the variations of signatures in space, is whether  
493 differences between catchments for a given signature truly reflect differences in  
494 hydrological processes, or rather, data and method uncertainties.

495  
496 Ideally, we would like signatures to provide insights into hydrological processes, in order  
497 to advance process understanding and modeling. But signatures are also influenced by  
498 how data are collected (Westerberg and McMillan, 2015; McMillan et al., 2017). For  
499 instance, the frequency of zero discharge is impacted by the fact that different stations  
500 report very low flows differently, which is likely to contribute to the strong variations in  
501 space (Figure 3i) and to partly explain why the random forest predictions and the SAC  
502 simulations are particularly poor for this signature (Figure 2). Further, the formulation of  
503 the signature influences its value, and if it is not robust enough, it can exacerbate  
504 insignificant differences or mask significant differences between catchments. For  
505 instance, streamflow-precipitation elasticity can be formulated in different ways, some  
506 being less sensitive to outliers (Sankarasubramanian et al., 2001). It is well possible that  
507 other signatures suffer from similar drawbacks: their aim is clear, but their formulation  
508 does not capture well that they should because it is lacking robustness.

509  
510 Note that uncertainties related to data and methods are only two factors making it  
511 difficult to isolate and understand differences in behavior between catchments. A more  
512 general issue is that, while signatures enable us to explore hydrological behavior, they do  
513 not necessarily allow us to pinpoint the hydrological processes leading to this behavior.  
514 For instance, the slope of the flow duration can be related to myriad of processes which  
515 are difficult to disentangle and which interact in complex ways. Similarly, both baseflow  
516 generation and the snow melt contribute to the slowly-varying part of a hydrograph, but  
517 discharge separation techniques used to compute the baseflow index (such as digital  
518 filters) are unable to distinguish between these two processes. Also, both  
519 evapotranspiration and loss to groundwater lead to low values of the runoff ratio, but the  
520 runoff ratio on its own does not inform us on this partitioning. Furthermore, statistics  
521 based on high discharge thresholds enable us to explore the frequency and amplitude of  
522 floods, but do not account for the different processes leading to floods. In most cases,  
523 signatures do not enable us to focus on a single process, but rather, reflect the interplay of  
524 several processes. As a consequence of this diversity of processes, it is difficult to  
525 establish clear links between landscape attributes and hydrological signatures.

526

527 There are few exceptions, for instance the seasonality of discharge is in many cases  
528 determined by the seasonality of precipitation and the eventual presence of snow, and the  
529 mean discharge is strongly controlled by the aridity (top of the signature table). But  
530 overall, the hydrological drivers of many signatures are still unclear. Hydrological  
531 signatures are promising tools, but the results showed here illustrate that research on  
532 hydrological signatures is still at an early stage, since we still do not understand many of  
533 them well enough to explain what is driving their changes in space. We think that this  
534 should make us re-evaluate what they tell us on hydrological processes. To give one  
535 example, the precipitation-discharge elasticity is commonly used for anticipate the future  
536 impact of climate change on discharge, yet even recent research recognizes that “it is  
537 difficult to identify physical reasons, for the spatial variations in elasticity values”  
538 (Andréassian et al., 2016). If we are not able to explain how elasticity changes in space, is  
539 it reasonable to rely on it to produce projections of discharge under future climate, that  
540 will potentially support decision-making on adaptation strategies? We recognize the  
541 value of assessing the sensitivity of discharge to precipitation, but we wonder whether  
542 sensitivity is correctly captured by this specific signature (and hence, how much faith we  
543 should put into it).

#### 544 **4.3 Hydrological signatures for model calibration and selection**

545 SAC performs overall better than the random forests (Figure 2). It captures very well the  
546 mean annual, winter and summer discharge, the half-flow date and the baseflow index.  
547 Q95 is also well captured, which should not come as a surprise since RMSE was used as  
548 objective function. Yet, our results reveal that other signatures, such as the low flows  
549 metrics, the slope of the flow duration curve and the discharge-streamflow elasticity are  
550 poorly captured. This reflects that using a general metric such as RMSE can deliver a  
551 good overall performance, but does not provide enough constrains to capture specific  
552 parts of the hydrograph, which may contain important information on catchment behavior  
553 (De Boer-Euser et al., 2017).

554  
555 To overcome this issue, an option is to use hydrological signatures in the parameter  
556 estimation process (e.g., Vrugt and Sadegh, 2013). It is not clear however, how these  
557 signatures should be selected. Based on the results presented in this study, we  
558 hypothesize that signatures from the bottom of the table shown in Figure 4 have relatively  
559 low value for model calibration if their uncertainties are not accounted for. These  
560 signatures can be strongly influenced by data and method uncertainties, so approaching  
561 them from a deterministic perspective and trying to exactly match them may not bring  
562 much, since it means using a hydrological model to mimic variations over space that are  
563 only partially related to hydrological processes. Again, in this study, we do not explicitly  
564 assess how data and formulation uncertainties propagate into the signatures. Yet, the  
565 wider range in the random forest predictions and the scatter in the maps of these  
566 signatures indicate that they are particularly uncertain. The signatures we identify as  
567 uncertain are also considered as uncertain by Westerberg et al. (2016). Future research  
568 should systematically assess the value of signatures. Model calibration using a wide  
569 range of signatures in a wide range of catchments would help us to better assess which  
570 signatures are most useful for hydrological calibration.

571

572 Our concerns about model calibration using signatures impacted by data and methods  
573 uncertainties also apply to model evaluation (and by extension, to model comparison).  
574 Signatures at the bottom of the table are particularly uncertain and their relationship to  
575 catchment characteristics remain elusive (i.e., we do not have a good handle on those  
576 signatures). To use an example, we can predict the mean discharge in space well, which  
577 provides us with a reference models can be compared to. In contrast, if we consider the  
578 slope of the flow duration curve, it is poorly constrained by observations. Although we  
579 can compute its value, we cannot explain its variations in space, hence we question  
580 whether this reference is robust enough to enable model comparison. In absence of  
581 uncertainty estimates, we do not think that a model should be selected instead of another  
582 model, based solely on its better representation of signatures from the bottom of the table.

## 583 **5 Conclusions and outlook**

584

585 We systematically explored how landscape attributes influence (or not) hydrological  
586 signatures. We described the landscape of 671 catchments in the contiguous USA using  
587 five classes of attributes (topography, climatology, land cover, soil and geology) and  
588 summarized catchment behaviour using 15 hydrological signatures. Random forests  
589 allowed us to combine those landscape characteristics in non-linear ways and to  
590 quantitatively explore their relative influence on hydrological signatures. We found that  
591 climatic attributes are by far the most influential predictors for signatures that can be  
592 well-predicted based on catchment attributes (such as the mean annual discharge or the  
593 half-flow date), with land cover, soil and geology attributes playing secondary roles. Yet,  
594 several other signatures, such as the slope of the flow duration curve or the streamflow-  
595 precipitation elasticity are poorly predicted based on catchments attributes, and in  
596 particular, could not be satisfactorily predicted by climatic indices alone.

597

598 Using a large sample of catchments enabled us to explore the spatial patterns of  
599 hydrological signatures over the CONUS, and to characterize their spatial smoothness  
600 (auto-correlation) using Moran's  $I$ . We found that spatial smoothness is a simple yet  
601 powerful way to gain insights into a variety of aspects of large-sample studies. Signatures  
602 with smooth spatial variations are typically those with a high spatial predictability. In  
603 contrast, when signatures exhibit abrupt changes over short distances, those changes  
604 usually cannot be related to catchment attributes using random forests and they are also  
605 poorly captured by hydrological simulations from a conceptual model. Those sudden  
606 variations make signature regionalization difficult if neighbouring catchments are used as  
607 donors. The reasons behind noisy spatial patterns are not entirely clear and deserve more  
608 attention.

609

610 In summary, we found strong relationships between i) our ability to capture hydrological  
611 signatures using simulations from a conceptual hydrological model (SAC), ii) our ability  
612 to predict them using catchment characteristics as predictors in a machine-learning  
613 algorithm (random forests), iii) the spatial smoothness of the maps of these signatures  
614 (characterized using Moran's  $I$ ) and iv) the strength of the climate influence on those  
615 signatures. The strong consistency between these four aspects enabled us to rank  
616 hydrological signatures (Figure 4). Signatures at the bottom of this ranking are poorly

617 related to catchment attributes, poorly captured by SAC, their spatial pattern is noisy, and  
618 based on results from other studies, they are also particularly susceptible to discharge  
619 uncertainties and difficult to regionalize. In other words, these signatures are poorly  
620 constrained by discharge observations and the drivers of their variations in space are  
621 elusive. Hence in absence of uncertainty estimates for these signatures, we question their  
622 reliability to formulate conclusions on hydrological processes and we do not recommend  
623 them for the evaluation and selection of hydrological models. Those findings are outlined  
624 in Table 3.

625

626 Future research could explore whether signatures at the top of the ranking deliver better  
627 results when used for the calibration and selection of hydrological models. Another  
628 research avenue would be to re-use the framework presented here and explore how our  
629 conclusions vary when a subsample of catchments is selected in order to explore a  
630 specific landscape feature. We hope that the ideas and results presented in this study will  
631 trigger discussions on the drivers of hydrological processes at the catchment scale and on  
632 the use of hydrological signatures for hydrological modeling.

### 633 **Appendix 1: An introduction to regression trees and random forests**

634

635 We chose to use a machine-learning tool (random forests, Breiman, 2001) to explore how  
636 the interplay between landscape attributes shapes hydrological behavior. Machine-  
637 learning algorithms are gaining in popularity as the quantity and diversity of data to  
638 process increase. Machine-learning algorithms have been shown to be powerful  
639 prediction techniques, including in hydrologic studies (e.g., Gudmundsson and  
640 Seneviratne, 2013; Beck et al., 2015). Here we present a brief introduction to random  
641 forests, which may be useful for the interpretation of our results.

642

643 A random forest relies on an ensemble of regression trees to relate predictors (here  
644 catchment attributes) to a response variable (here a hydrological signature). In a  
645 regression tree, the prediction is made based on a series of threshold-based conditions on  
646 the predictors. The prediction scheme is initiated at the top of the tree (in the example  
647 shown in Figure A1a, the question at the top split is whether the mean elevation is greater  
648 than 1151m). The prediction is then refined using other thresholds on other (and  
649 sometimes the same) predictors at lower levels of the tree. The influence of each  
650 predictor on the response variable can be estimated based on its position in the regression  
651 tree: predictors appearing higher in the tree have a higher separating/predictive power  
652 (Figure A1a indicates that mean elevation is a strong predictor of the base flow index,  
653 likely because it conditions the formation a snow pack, which will increase the baseflow  
654 index when it melts). Note that regression trees are typically not symmetrical (different  
655 variables are used in different parts of the tree).

656

657 Regression trees are grown following a “recursive binary splitting” approach. The  
658 procedure starts at the top of the tree and at each split, one variable and one threshold are  
659 selected in order to minimize the mean squared error (MSE) of the prediction. The  
660 prediction is the mean value of the predictor for all the elements (catchments) falling in  
661 each class. As a consequence, the predictions of a decision tree are discrete values (one

662 per terminal node, such as 0.4801 for the left-most terminal node of the tree shown in  
663 Figure A1a, which leads to the horizontally aligned back points in Figure A1b). Trees are  
664 grown and then pruned by minimizing the cross-validated MSE in order to reduce the risk  
665 of overfitting. While regression trees are intuitive to interpret and can deal with non-  
666 linear relationships between variables, they typically lack robustness. We found that  
667 regression trees produced by randomly excluding half of the catchments to be quite  
668 different in the predictive variables they selected and in the position of these variables in  
669 the tree.

670

671 To overcome this limitation, we used random forests instead of single regression trees.  
672 Random forests are an ensemble of regression trees (here we used 500 trees per forest).  
673 The robustness of the forest comes from the way each tree is grown. At each split, a  
674 subsample of predictors is randomly excluded and the prediction must be done using  
675 solely the remaining. This implies that strong predictors, which otherwise might have  
676 been used for this specific split, will be excluded. This introduces differences between the  
677 trees, making the prediction more robust than if all the trees were similar. The number of  
678 trees  $N$  and the number of predictors  $P$  excluded at each split are variables defined by the  
679 user. We found that variations around the default value for  $P$  (a third of the total number  
680 of predictors) has little influence on our predictions, and that  $N = 500$  is adequate because  
681 it leads to better predictions than small forests, but more trees did not improve the  
682 predictions.

683

684 Since it is not practical to inspect each tree to determine which variables are used for the  
685 prediction, the relative influence of the predictors of a random forest is measured in an  
686 automated way. Once the forest has been grown, each predictor is considered individually  
687 and its values are shuffled (their statistical distribution remains the same but their order is  
688 now random). The relative drop in prediction accuracy (expressed in %) indicates how  
689 influential this predictor is (large increases in MSE indicate influential predictors). Figure  
690 A1c shows that for the prediction of the baseflow by a random forest, the fraction of  
691 precipitation falling as snow is the most influential predictor.

692 An advantage of growing a random forest is that the ensemble of trees can be used to  
693 characterize the uncertainty in the prediction. We used QQ plots to assess the reliability  
694 of the ensembles and found that for all the hydrological signatures except the fraction of  
695 no flow, the ensembles are remarkably reliable (Figure A1d). Although this is not a  
696 feature we use in this study, we consider important to stress this finding, as it can be  
697 relevant in other contexts, for instance for parameter estimation based on regionalized  
698 hydrological signatures. Finally, note that because the deterministic prediction of each  
699 random forest is the mean prediction of its regression trees, the predictions are continuous  
700 values. This reduces the granularity of the predictions when compared to regression trees,  
701 which only predict a limited number of discrete values (Figure A1b).

702

703 **Appendix 2: Moran's  $I$  as a measure of spatial smoothness**

704



705 When a variable is plotted on a map for numerous catchments, spatial patterns can appear  
706 and help with the formulation of starting hydrological hypotheses. A fundamental  
707 advantage of large-sample hydrology over small-sample hydrology is that, when maps  
708 are produced using hundreds of catchments, those insights are likely to be clearer than if  
709 the maps were based on a handful of catchments, because those tend to be patchier.

710

711 In this study, we explore and quantify regional variability in hydrological signatures  
712 using a measure of spatial smoothness. Addor et al. (2017b) observed that maps of  
713 climate indices generally exhibit smoother patterns than maps of hydrological signatures,  
714 whose patterns tend to be noisier (with potentially strong differences between adjacent  
715 catchments). Similar differences in spatial variability can also be observed among  
716 hydrological signatures: some signatures vary gradually across the landscape, while  
717 others exhibit abrupt changes over short distances. This is already apparent in earlier  
718 studies. Figure 2 of Sawicz et al. (2011) indicates for instance that the runoff ratio over  
719 the Eastern United States varies more smoothly in space than the slope of the flow  
720 duration curve.

721

722 To quantify the smoothness of spatial patterns in maps of hydrological signatures, we  
723 measure the spatial autocorrelation using Moran's  $I$  (Moran, 1950; Legendre and  
724 Legendre, 1998):

725

$$726 \quad I = \frac{\frac{1}{W} \sum_{i=1}^N \sum_{j=1}^N w_{i,j} (x_i - \bar{x})(x_j - \bar{x})}{\frac{1}{N} \sum_{i=1}^N (x_i - \bar{x})^2}$$

727

728 where  $x$  is the variable of interest with  $N$  elements (here  $N = 671$  catchments),  $\bar{x}$  is its  
729 mean,  $w$  is the weight associated with each pair of catchments (here  $w = 1/d$ , where  $d$  is  
730 the distance along a great circle between the two catchments, the diagonal elements of the  
731 matrix  $w$  being set to 0) and  $W$  is the sum of all the weights. Spatial correlation can be  
732 related to temporal autocorrelation: if all the pairs of data points close in space (in time)  
733 have a similar value, then the field is spatially (temporally) auto-correlated. Differences  
734 (or similarities) between points far apart have a comparatively small influence on  $I$   
735 because of the distance-based weighting system selected.  $I$  values close to 0 indicate no  
736 spatial correlation. The higher the value  $I$ , the greater the spatial auto-correlation and the  
737 smoother the spatial patterns (compare Figures 2a, e and i for an example). Note that in  
738 contrast to correlation coefficients,  $|I|$  can exceed 1 (de Jong et al., 1984).

### 739 **Acknowledgements**

740

741 This work was supported by the US Army Corps of Engineers Climate Preparedness and  
742 Resilience programs. The National Center for Atmospheric Research (NCAR) is  
743 sponsored by the US National Science Foundation. Funding from the Swiss National  
744 Science Foundation is acknowledged (grant P2ZHP2\_161963). We thank Pablo Mendoza  
745 for recommending QQplots for the evaluation of the random forest. The CAMELS  
746 hydrometeorological time series (<https://doi.org/10.5065/D6MW2F4D>) and attributes

747 (<https://doi.org/10.5065/D6G73C3Q>, version 2.1 is used in this study) are freely available  
748 online.

749 **References**

750

751 Addor, N., Newman, A. J., Mizukami, N. and Clark, M. P.: Catchment attributes for  
752 large-sample studies, , doi:10.5065/D6G73C3Q, 2017a.

753 Addor, N., Newman, A. J., Mizukami, N. and Clark, M. P.: The CAMELS data set:  
754 catchment attributes and meteorology for large-sample studies, *Hydrol. Earth Syst. Sci.*,  
755 21(10), 5293–5313, doi:10.5194/hess-21-5293-2017, 2017b.

756 Almeida, S. L., Bulygina, N., McIntyre, N., Wagener, T. and Buytaert, W.: Predicting  
757 flows in ungauged catchments using correlated information sources, *Proc. Br. Hydrol.*  
758 *Soc. Elev. Natl. Symp. Hydrol. a Chang. world*, Dundee, July 2012, 1–7,  
759 doi:10.7558/bhs.2012.ns02, 2012.

760 Almeida, S., Le Vine, N., McIntyre, N., Wagener, T. and Buytaert, W.: Accounting for  
761 dependencies in regionalized signatures for predictions in ungauged catchments, *Hydrol.*  
762 *Earth Syst. Sci.*, 20(2), 887–901, doi:10.5194/hess-20-887-2016, 2016.

763 Anderson, E. A.: National Weather Service River Forecast System - Snow accumulation  
764 and ablation model, *Tech. Memo. NWS HYDRO-17.*, 1973.

765 Andréassian, V., Coron, L., Lerat, J. and Le Moine, N.: Climate elasticity of streamflow  
766 revisited - An elasticity index based on long-term hydrometeorological records, *Hydrol.*  
767 *Earth Syst. Sci.*, 20(11), 4503–4524, doi:10.5194/hess-20-4503-2016, 2016.

768 Beck, H. E., de Roo, A. and van Dijk, A. I. J. M.: Global maps of streamflow  
769 characteristics based on observations from several thousand catchments, *J.*  
770 *Hydrometeorol.*, 150423121816007, doi:10.1175/JHM-D-14-0155.1, 2015.

771 Berghuijs, W. R., Sivapalan, M., Woods, R. A. and Savenije, H. H. G.: Patterns of  
772 similarity of seasonal water balances: A window into streamflow variability over a range  
773 of time scales, *Water Resour. Res.*, 50, 5638–5661, doi:10.1002/2014WR015692, 2014.

774 De Boer-Euser, T., Bouaziz, L., De Niel, J., Brauer, C., Dewals, B., Drogue, G., Fenicia,  
775 F., Grelier, B., Nossent, J., Pereira, F., Savenije, H., Thirel, G. and Willems, P.: Looking  
776 beyond general metrics for model comparison - Lessons from an international model  
777 intercomparison study, *Hydrol. Earth Syst. Sci.*, 21, 423–440, doi:10.5194/hess-21-423-  
778 2017, 2017.

779 Breiman, L.: Random forests, *Mach. Learn.*, 45(1), 5–32, doi:10.1023/A:1010933404324,  
780 2001.

781 Budyko, M. I.: *Climate and life*, New York Academic Press., 1974.

782 Burnash, R. J. C., Ferral, R. L. and McGuire, R. A.: A generalized streamflow simulation  
783 system: Conceptual modeling for digital computers., 1973.

784 Chaney, N. W., Wood, E. F., McBratney, A. B., Hempel, J. W., Nauman, T. W.,  
785 Brungard, C. W. and Odgers, N. P.: POLARIS: A 30-meter probabilistic soil series map  
786 of the contiguous United States, *Geoderma*, 274, 54–67,  
787 doi:10.1016/j.geoderma.2016.03.025, 2016.

788 Chiverton, A., Hannaford, J., Holman, I., Corstanje, R., Prudhomme, C., Bloomfield, J.  
789 and Hess, T. M.: Which catchment characteristics control the temporal dependence  
790 structure of daily river flows?, *Hydrol. Process.*, 29(6), 1353–1369,  
791 doi:10.1002/hyp.10252, 2015.

- 792 Clark, M. P., McMillan, H. K., Collins, D. B. G., Kavetski, D. and Woods, R. A.:  
793 Hydrological field data from a modeller's perspective: Part 2: Process-based evaluation  
794 of model hypotheses, *Hydrol. Process.*, 25(4), 523–543, doi:10.1002/hyp.7902, 2011.
- 795 Clausen, B. and Biggs, B. J. F.: Flow variables for ecological studies in temperate  
796 streams: Groupings based on covariance, *J. Hydrol.*, 237(3–4), 184–197,  
797 doi:10.1016/S0022-1694(00)00306-1, 2000.
- 798 Cosby, B. J., Hornberger, G. M., Clapp, R. B. and Ginn, T. R.: A Statistical Exploration  
799 of the Relationships of Soil Moisture Characteristics to the Physical Properties of Soils,  
800 *Water Resour. Res.*, 20(6), 682–690, doi:10.1029/WR020i006p00682, 1984.
- 801 Court, A.: Measures of streamflow timing, *J. Geophys. Res.*, 67(11), 4335–4339,  
802 doi:10.1029/JZ067i011p04335, 1962.
- 803 Crawford, N. H. and Linsley, R. K.: Digital simulation in hydrology: Stanford Watershed  
804 Model IV., 1966.
- 805 Duan, Q., Sorooshian, S. and Gupta, H. V.: Effective and efficient global optimization for  
806 conceptual rainfall-runoff models, *Water Resour. Res.*, 28(4), 1015–1031,  
807 doi:10.1029/91WR02985, 1992.
- 808 Euser, T., Winsemius, H. C., Hrachowitz, M., Fenicia, F., Uhlenbrook, S. and Savenije,  
809 H. H. G.: A framework to assess the realism of model structures using hydrological  
810 signatures, *Hydrol. Earth Syst. Sci.*, 17(5), 1893–1912, doi:10.5194/hess-17-1893-2013,  
811 2013.
- 812 Falcone, J. A.: GAGES-II: Geospatial Attributes of Gages for Evaluating Streamflow.  
813 [online] Available from:  
814 [https://water.usgs.gov/GIS/metadata/usgswrd/XML/gagesII\\_Sept2011.xml](https://water.usgs.gov/GIS/metadata/usgswrd/XML/gagesII_Sept2011.xml), 2011.
- 815 Gleeson, T., Moosdorf, N., Hartmann, J. and van Beek, L. P. H.: A glimpse beneath  
816 earth's surface: GLobal HYdrogeology MaPS (GLHYMPS) of permeability and porosity,  
817 *Geophys. Res. Lett.*, 41, 3891–3898, doi:10.1002/2014GL059856, 2014.
- 818 Gudmundsson, L. and Seneviratne, S. I.: Do land parameters matter in large-scale  
819 terrestrial water dynamics? – Toward new paradigms in modelling strategies, *Hydrol.*  
820 *Earth Syst. Sci. Discuss.*, 10(11), 13191–13229, doi:10.5194/hessd-10-13191-2013, 2013.
- 821 Gupta, H. V., Wagener, T. and Liu<sup>1</sup>, Y.: Reconciling theory with observations: elements  
822 of a diagnostic approach to model evaluation, *Hydrol. Process.*, 22, 3802–3813,  
823 doi:10.1002/hyp.6989, 2008.
- 824 Harman, C. and Troch, P. A.: What makes Darwinian hydrology “darwinian”? Asking a  
825 different kind of question about landscapes, *Hydrol. Earth Syst. Sci.*, 18(2), 417–433,  
826 doi:10.5194/hess-18-417-2014, 2014.
- 827 Hartmann, J. and Moosdorf, N.: The new global lithological map database GLiM: A  
828 representation of rock properties at the Earth surface, *Geochemistry, Geophys.*  
829 *Geosystems*, 13(12), 1–37, doi:10.1029/2012GC004370, 2012.
- 830 Hengl, T., Mendes De Jesus, J., Heuvelink, G. B. M., Gonzalez, M. R., Kilibarda, M.,  
831 Blagotić, A., Shangguan, W., Wright, M. N., Geng, X., Bauer-Marschallinger, B.,  
832 Guevara, M. A., Vargas, R., MacMillan, R. A., Batjes, N. H., Leenaars, J. G. B., Ribeiro,  
833 E., Wheeler, I., Mantel, S. and Kempen, B.: SoilGrids250m: Global Gridded Soil  
834 Information Based on Machine Learning, *PLoS One*, 12(2), e0169748,  
835 doi:10.1371/journal.pone.0169748, 2017.
- 836 Hrachowitz, M., Fovet, O., Ruiz, L., Euser, T., Gharari, S., Nijzink, R., Freer, J.,  
837 Savenije, H. H. G. and Gascuel-Oudou, C.: Process consistency in models: The

- 838 importance of system signatures, expert knowledge, and process complexity, , 7206–  
839 7230, doi:10.1002/2013WR014956.Received, 2014.
- 840 Hrachowitz, M., Savenije, H. H. G., Blöschl, G., McDonnell, J. J., Sivapalan, M.,  
841 Pomeroy, J. W., Arheimer, B., Blume, T., Clark, M. P., Ehret, U., Fenicia, F., Freer, J. E.,  
842 Gelfan, A., Gupta, H. V., Hughes, D. a., Hut, R. W., Montanari, A., Pande, S., Tetzlaff,  
843 D., Troch, P. a., Uhlenbrook, S., Wagener, T., Winsemius, H. C., Woods, R. a., Zehe, E.  
844 and Cudennec, C.: A decade of Predictions in Ungauged Basins (PUB)—a review,  
845 *Hydrol. Sci. J.*, 58(6), 1198–1255, doi:10.1080/02626667.2013.803183, 2013.
- 846 James, G., Witten, D., Hastie, T. and Tibshirani, R.: *An Introduction to Statistical*  
847 *Learning with Applications in R*, edited by Springer., 2013.
- 848 de Jong, P., Sprenger, C. and van Veen, F.: On Extreme Values of Moran’s I and Geary’s  
849 c, *Geogr. Anal.*, 16(1), 17–24, doi:10.1111/j.1538-4632.1984.tb00797.x, 1984.
- 850 Kuentz, A., Arheimer, B., Hundecha, Y. and Wagener, T.: Understanding hydrologic  
851 variability across Europe through catchment classification, *Hydrol. Earth Syst. Sci.*, 21,  
852 2863–2879, doi:10.5194/hess-21-2863-2017, 2017.
- 853 Ladson, A., Brown, R., Neal, B. and Nathan, R.: A standard approach to baseflow  
854 separation using the Lyne and Hollick filter, *Aust. J. Water Resour.*, 17(1), 25–34,  
855 doi:http://dx.doi.org/10.7158/W12-028.2013.17.1., 2013.
- 856 Laio, F. and Tamea, S.: Verification tools for probabilistic forecasts of continuous  
857 hydrological variables, *Hydrol. Earth Syst. Sci.*, 11(4), 1267–1277, doi:10.5194/hess-11-  
858 1267-2007, 2007.
- 859 Lawrence, D. M. and Slater, A. G.: Incorporating organic soil into a global climate  
860 model, *Clim. Dyn.*, 30(2–3), 145–160, doi:10.1007/s00382-007-0278-1, 2008.
- 861 Legendre, P. and Legendre, L.: *Numerical ecology*, Elsevier, New York., 1998.
- 862 Liaw, A. and Wiener, M.: Classification and Regression by randomForest, *R News*, 2(3),  
863 18–22, 2002.
- 864 McMillan, H. K., Clark, M. P., Bowden, W. B., Duncan, M. and Woods, R. A.:  
865 Hydrological field data from a modeller’s perspective: Part 1. Diagnostic tests for model  
866 structure, *Hydrol. Process.*, 25(4), 511–522, doi:10.1002/hyp.7841, 2011.
- 867 McMillan, H., Westerberg, I. and Branger, F.: Five guidelines for selecting hydrological  
868 signatures, *Hydrol. Process.*, 1–5, doi:10.1002/hyp.11300, 2017.
- 869 Miller, D. A. and White, R. A.: A Conterminous United States Multilayer Soil  
870 Characteristics Dataset for Regional Climate and Hydrology Modeling, *Earth Interact.*,  
871 2(2), doi:10.1175/1087-3562(1998)002<0002:CUSMS>2.0.CO;2, 1998.
- 872 Moran, P. A. P.: Notes on Continuous Stochastic Phenomena, *Biometrika*, 37(1/2), 17,  
873 doi:10.2307/2332142, 1950.
- 874 Newman, A. J., Clark, M. P., Sampson, K., Wood, A., Hay, L. E., Bock, A., Viger, R.,  
875 Blodgett, D., Brekke, L., Arnold, J. R., Hopson, T. and Duan, Q.: Development of a  
876 large-sample watershed-scale hydrometeorological dataset for the contiguous USA:  
877 dataset characteristics and assessment of regional variability in hydrologic model  
878 performance, *Hydrol. Earth Syst. Sci.*, 19, 209–223, doi:10.5194/hess-19-209-2015,  
879 2015.
- 880 Newman, A. J., Sampson, K., Clark, M. P., Bock, A., Viger, R. J. and Blodgett, D.: A  
881 large sample watershed-scale hydrometeorological dataset for the contiguous USA, ,  
882 doi:10.5065/D6MW2F4D, 2014.
- 883 Olden, J. D. and Poff, N. L.: Redundancy and the choice of hydrologic indices for

- 884 characterizing streamflow regimes, *River Res. Appl.*, 19(2), 101–121,  
885 doi:10.1002/rra.700, 2003.
- 886 Padrón, R. S., Gudmundsson, L., Greve, P. and Seneviratne, S. I.: Large-Scale Controls  
887 of the Surface Water Balance Over Land: Insights From a Systematic Review and Meta-  
888 Analysis, *Water Resour. Res.*, 1–20, doi:10.1002/2017WR021215, 2017.
- 889 Pelletier, J. D., Patrick D. Broxton, Hazenberg, P., Zeng, X., Troch, P. A., Niu, G.-Y.,  
890 Williams, Z., Brunke, M. A. and Gochis, D.: A gridded global data set of soil, intact  
891 regolith, and sedimentary deposit thicknesses for regional and global land surface  
892 modeling, *J. Adv. Model. Earth Syst.*, 8, doi:10.1002/2015MS000526, 2016.
- 893 Priestley, C. H. B. and Taylor, R. J.: On the Assessment of Surface Heat Flux and  
894 Evaporation Using Large-Scale Parameters, *Mon. Weather Rev.*, 100(February), 81–92,  
895 doi:10.1175/1520-0493(1972)100<0081:OTAOSH>2.3.CO;2, 1972.
- 896 R Core Team: R: A Language and Environment for Statistical Computing, [online]  
897 Available from: <http://www.r-project.org/>, 2017.
- 898 Rakovec, O., Kumar, R., Mai, J., Cuntz, M., Thober, S., Zink, M., Attinger, S., Schäfer,  
899 D., Schrön, M. and Samaniego, L.: Multiscale and Multivariate Evaluation of Water  
900 Fluxes and States over European River Basins, *J. Hydrometeorol.*, 17(1), 287–307,  
901 doi:10.1175/JHM-D-15-0054.1, 2016.
- 902 Renard, B., Kavetski, D., Kuczera, G., Thyer, M. and Franks, S. W.: Understanding  
903 predictive uncertainty in hydrologic modeling: The challenge of identifying input and  
904 structural errors, *Water Resour. Res.*, 46(5), 1–22, doi:10.1029/2009WR008328, 2010.
- 905 Rice, J. S., Emanuel, R. E. and Vose, J. M.: The influence of watershed characteristics on  
906 spatial patterns of trends in annual scale streamflow variability in the continental U.S., *J.*  
907 *Hydrol.*, 540, 850–860, doi:10.1016/j.jhydrol.2016.07.006, 2016.
- 908 Samaniego, L., Kumar, R. and Attinger, S.: Multiscale parameter regionalization of a  
909 grid-based hydrologic model at the mesoscale, *Water Resour. Res.*, 46(5),  
910 doi:10.1029/2008WR007327, 2010.
- 911 Sankarasubramanian, A., Vogel, R. M. and Limbrunner, J. F.: Climate elasticity of  
912 streamflow in the United States, *Water Resour. Res.*, 37(6), 1771–1781,  
913 doi:10.1029/2000WR900330, 2001.
- 914 Sawicz, K., Wagener, T., Sivapalan, M., Troch, P. a. and Carrillo, G.: Catchment  
915 classification: Empirical analysis of hydrologic similarity based on catchment function in  
916 the eastern USA, *Hydrol. Earth Syst. Sci.*, 15(9), 2895–2911, doi:10.5194/hess-15-2895-  
917 2011, 2011.
- 918 Singh, R., Archfield, S. A. and Wagener, T.: Identifying dominant controls on hydrologic  
919 parameter transfer from gauged to ungauged catchments - A comparative hydrology  
920 approach, *J. Hydrol.*, 517, 985–996, doi:10.1016/j.jhydrol.2014.06.030, 2014.
- 921 Snelder, T. H., Lamouroux, N., Leathwick, J. R., Pella, H., Sauquet, E. and Shankar, U.:  
922 Predictive mapping of the natural flow regimes of France, *J. Hydrol.*, 373(1–2), 57–67,  
923 doi:10.1016/j.jhydrol.2009.04.011, 2009.
- 924 Thornton, P. E., Thornton, M. M., Mayer, B. W., Wilhelmi, N., Wei, Y. and Cook, R. B.:  
925 Daymet: Daily surface weather on a 1km grid for North America, 1980–2012., 2012.
- 926 Troch, P. A., Martinez, G. F., Pauwels, V. R. N., Durcik, M., Sivapalan, M., Harman, C.,  
927 Brooks, P. D., Gupta, H. and Huxman, T.: Climate and vegetation water use efficiency at  
928 catchment scales, *Hydrol. Process.*, 23, 2409–2414, doi:10.1002/hyp.7358, 2009.
- 929 Viger, R. J. and Bock, A.: GIS Features of the Geospatial Fabric for National Hydrologic

930 Modeling., 2014.  
931 Vrugt, J. A. and Sadegh, M.: Toward diagnostic model calibration and evaluation:  
932 Approximate Bayesian computation, *Water Resour. Res.*, 49(7), 4335–4345,  
933 doi:10.1002/wrcr.20354, 2013.  
934 Westerberg, I. K. and McMillan, H. K.: Uncertainty in hydrological signatures, *Hydrol.*  
935 *Earth Syst. Sci.*, 19(9), 3951–3968, doi:10.5194/hess-19-3951-2015, 2015.  
936 Westerberg, I. K., Wagener, T., Coxon, G., McMillan, H. K., Castellarin, A., Montanari,  
937 A. and Freer, J.: Uncertainty in hydrological signatures for gauged and ungauged  
938 catchments, *Water Resour. Res.*, 52, 1847–1865, doi:10.1002/2015WR017635, 2016.  
939 Woods, R. A.: Analytical model of seasonal climate impacts on snow hydrology:  
940 Continuous snowpacks, *Adv. Water Resour.*, 32, 1465–1481,  
941 doi:10.1016/j.advwatres.2009.06.011, 2009.  
942 Yilmaz, K. K., Gupta, H. V. and Wagener, T.: A process-based diagnostic approach to  
943 model evaluation: Application to the NWS distributed hydrologic model, *Water Resour.*  
944 *Res.*, 44(May), 1–18, doi:10.1029/2007WR006716, 2008.  
945 Zeng, X.: Global Vegetation Root Distribution for Land Modeling, *J. Hydrometeorol.*,  
946 2(5), 525–530, doi:10.1175/1525-7541(2001)002<0525:GVRDFL>2.0.CO;2, 2001.  
947  
948  
949  
950  
951

952 **Table 1: Catchment attributes**  
 953

<b>camels_topo - Topography and location</b>			
<b>Description</b>	<b>Unit</b>	<b>Data source</b>	<b>References</b>
gauge latitude	° north	N15 - USGS data	
gauge longitude	° east	N15 - USGS data	
catchment mean elevation	meter above sea level	N15 - USGS data	
catchment mean slope	m/km	N15 - USGS data	
catchment area (GAGESII estimate)	km <sup>2</sup>	N15 - USGS data	Falcone (2011)
catchment area (Geospatial Fabric estimate)	km <sup>2</sup>	N15 - Geospatial Fabric	Viger (2014), Viger and Bock (2014)
<b>camels_clim - Climate indices - *: Computed over the period 1989/10/01 to 2009/09/30</b>			
<b>Description</b>	<b>Unit</b>	<b>Data source</b>	<b>References</b>
mean daily precipitation	mm/day	N15 - Daymet*	
mean daily PET [estimated by N15 using Priestley-Taylor formulation calibrated for each catchment]	mm/day	N15 - Daymet*	
aridity (PET/P, ratio of mean PET [estimated by N15 using Priestley-Taylor formulation calibrated for each catchment] to mean precipitation)	-	N15 - Daymet*	
seasonality and timing of precipitation (estimated using sine curves to represent the annual temperature and precipitation cycles, positive [negative] values indicate that precipitation peaks in summer [winter], values close to 0 indicate uniform precipitation throughout the year)	-	N15 - Daymet*	Eq. 14 in Woods et al. (2009)
fraction of precipitation falling as snow (i.e., on days colder than 0°C)	-	N15 - Daymet*	
frequency of high precipitation days (>= 5 times mean daily precipitation)	days/year	N15 - Daymet*	
average duration of high precipitation events (number of consecutive days >= 5 times mean daily precipitation)	days	N15 - Daymet*	
season during which most high precipitation days (>= 5 times mean daily precip.) occur	season	N15 - Daymet*	
frequency of dry days (<1 mm/day)	days/year	N15 - Daymet*	
average duration of dry periods (number of consecutive days <1 mm/day)	days	N15 - Daymet*	
season during which most dry days (<1 mm/day) occur	season	N15 - Daymet*	
<b>camels_vege - Land cover characteristics - *: Period 2002 to 2014</b>			
<b>Description</b>	<b>Unit</b>	<b>Data source</b>	<b>References</b>
forest fraction	-	N15 - USGS data	
maximum monthly mean of the leaf area index (based on 12 monthly means)	-	MODIS*	
difference between the maximum and minimum monthly mean of the leaf area index (based on 12 monthly means)	-	MODIS*	
maximum monthly mean of the green vegetation fraction (based on 12 monthly means)	-	MODIS*	
difference between the maximum and minimum monthly mean of the green vegetation fraction (based on 12 monthly means)	-	MODIS*	
dominant land cover type (Noah-modified 20-category IGBP-MODIS land cover)	-	MODIS*	
fraction of the catchment area associated with the dominant land cover	-	MODIS*	
root depth (percentiles XX = 50 and 99% extracted from a root depth distribution based on IGBP land cover)	m	MODIS*	Eq. 2 and Table 2 in Zeng (2001)

954

955  
956  
957  
958

**Table 1 continued: Catchment attributes**

<b>camels_soil - Soil characteristics - *: Only covers the top 1.5 m</b>			
<b>Description</b>	<b>Unit</b>	<b>Data source</b>	<b>References</b>
depth to bedrock (maximum 50m)	m	Pelletier et al.	
soil depth (maximum 1.5m, layers marked as water and bedrock were excluded)	m	Miller and White (1998) - STATSGO*	
volumetric porosity (saturated volumetric water content estimated using a multiple linear regression based on sand and clay fraction for the layers marked as USDA soil texture class and a default value [0.9] for layers marked as organic material, layers marked as water, bedrock and "other" were excluded)	-	Miller and White (1998) - STATSGO*	Table 4 in Cosby et al. (1984), Lawrence and Slater (2008)
saturated hydraulic conductivity (estimated using a multiple linear regression based on sand and clay fraction for the layers marked as USDA soil texture class and a default value [36cm/hr] for layers marked as organic material, layers marked as water, bedrock and "other" were excluded)	cm/hr	Miller and White (1998) - STATSGO*	Table 4 in Cosby et al. (1984), Lawrence and Slater (2008)
maximum water content (combination of porosity and soil_depth_statgso, layers marked as water, bedrock and "other" were excluded)	m	Miller and White (1998) - STATSGO*	
sand fraction (of the soil material smaller than 2 mm, layers marked as organic material, water, bedrock and "other" were excluded)	%	Miller and White (1998) - STATSGO*	
silt fraction (of the soil material smaller than 2 mm, layers marked as organic material, water, bedrock and "other" were excluded)	%	Miller and White (1998) - STATSGO*	
clay fraction (of the soil material smaller than 2 mm, layers marked as organic material, water, bedrock and "other" were excluded)	%	Miller and White (1998) - STATSGO*	
fraction of the top 1.5m marked as water (class 14 )	%	Miller and White (1998) - STATSGO*	
fraction of soil_depth_statgso marked as organic material (class 13)	%	Miller and White (1998) - STATSGO*	
fraction of soil_depth_statgso marked as other (class 16)	%	Miller and White (1998) - STATSGO*	
<b>camels_geol - Geological characteristics</b>			
<b>Description</b>	<b>Unit</b>	<b>Data source</b>	<b>References</b>
most common geologic class in the catchment	-	GLIM	Hartmann and Moosdorf (2012)
fraction of the catchment area associated with its most common geologic class	-	GLIM	Hartmann and Moosdorf (2012)
2nd most common geologic class in the catchment	-	GLIM	Hartmann and Moosdorf (2012)
fraction of the catchment area associated with its 2nd most common geologic class	-	GLIM	Hartmann and Moosdorf (2012)
fraction of the catchment area characterized as "Carbonate sedimentary rocks"	-	GLIM	Hartmann and Moosdorf (2012)
subsurface porosity	-	GLHYMPS	Gleeson et al. (2014)
subsurface permeability (log10)	m <sup>2</sup>	GLHYMPS	Gleeson et al. (2014)

959



960 **Table 2: Hydrological signatures**  
 961

camels_hydro - Hydrological signatures - *: Period 1989/10/01 to 2009/09/30			
<i>Description</i>	<i>Unit</i>	<i>Data source</i>	<i>References</i>
mean annual discharge	mm/day	N15 - USGS data*	
mean winter (DJF) discharge	mm/day	N15 - USGS data*	
mean summer (JJA) discharge	mm/day	N15 - USGS data*	
runoff ratio (ratio of mean daily discharge to mean daily precipitation)	-	N15 - USGS data*	Eq. 2 in Sawicz et al. (2011)
streamflow-precipitation elasticity (sensitivity of streamflow to changes in precipitation at the annual time scale)	-	N15 - USGS data*	Eq. 7 in Sankarasubramanian et al. (2001), the last element being P/Q not Q/P
slope of the flow duration curve (between the log-transformed 33rd and 66th streamflow percentiles)		N15 - USGS data*	Eq. 3 in Sawicz et al. (2011)
baseflow index (ratio of mean daily baseflow to mean daily discharge, hydrograph separation performed using Ladson et al. [2013] digital filter)	-	N15 - USGS data*	Ladson et al. (2013)
mean half flow date (date on which the cumulative discharge since October 1st reaches half of the annual discharge)	day of year	N15 - USGS data*	Court (1962)
5% flow quantile (low flow)	mm/day	N15 - USGS data*	
95% flow quantile (high flow)	mm/day	N15 - USGS data*	
frequency of high-flow days (> 9 times the median daily flow)	days/year	N15 - USGS data*	Clausen and Biggs (2000), Table 2 in Westerberg and McMillan (2015)
mean duration of high-flow events (number of consecutive days > 9 times the median daily flow)	days	N15 - USGS data*	Clausen and Biggs (2000), Table 2 in Westerberg and McMillan (2015)
frequency of low-flow days (< 0.2 times the mean daily flow)	days/year	N15 - USGS data*	Olden and Poff (2003), Table 2 in Westerberg and McMillan (2015)
mean duration of low-flow events (number of consecutive days < 0.2 times the mean daily flow)	days	N15 - USGS data*	Olden and Poff (2003), Table 2 in Westerberg and McMillan (2015)
frequency of days with Q = 0 mm/day	%	N15 - USGS data*	

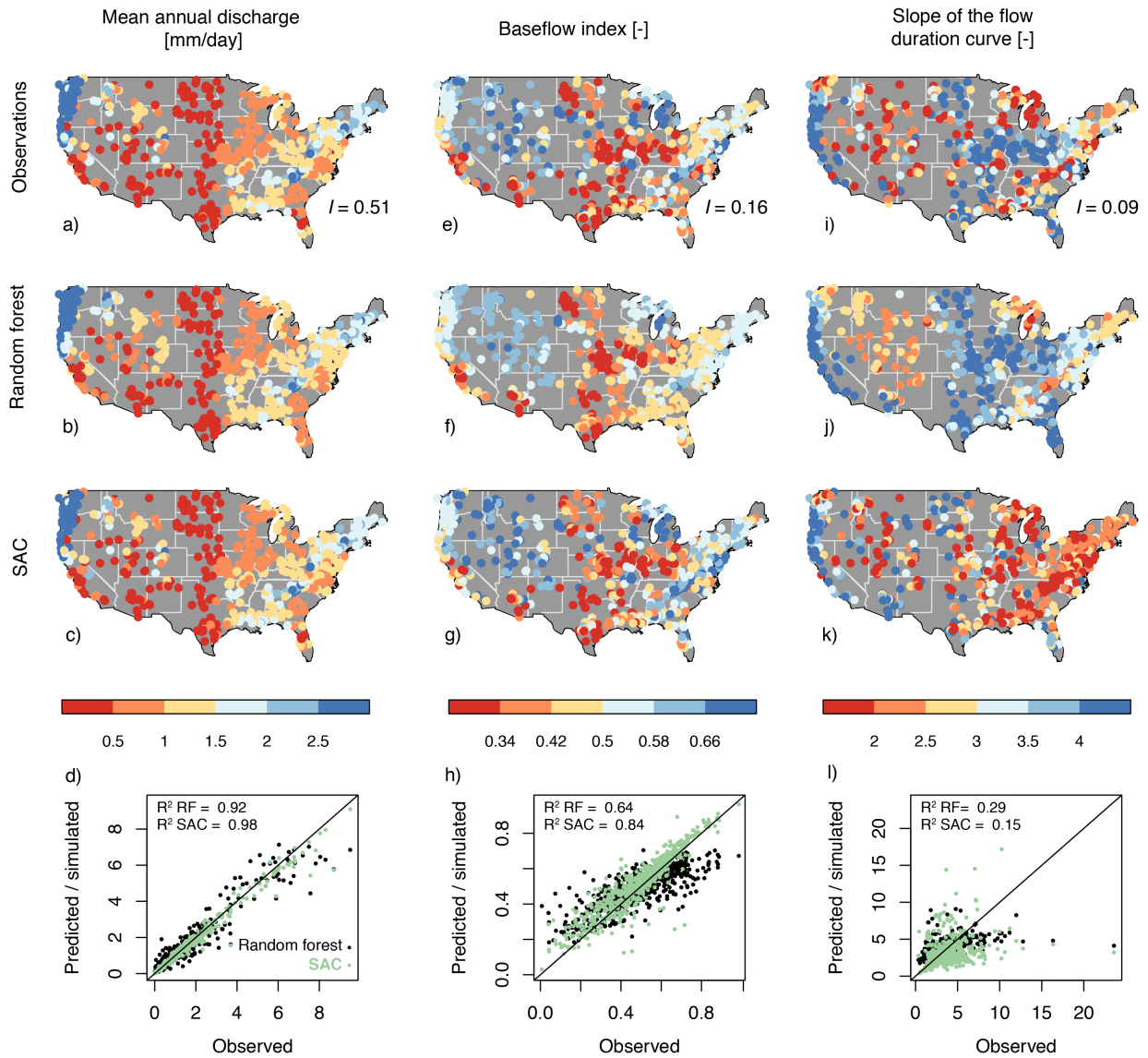
962  
 963

964 **Table 3: Summary of the typical differences between signatures from the top and**  
 965 **bottom of the signature table shown in Figure 4**

<b>Feature</b>	<b>Top of the table</b>	<b>Bottom of the table</b>	<b>Discussed in paper section</b>
<b>Results</b>			
Prediction by SAC	Good	Poor	3.1 and 3.2
Prediction by random forest	Good	Poor	3.1 and 3.2
Spatial field	Smooth	Noisy	3.1 and 3.2
Well constrained by climatic indices	Yes	No	3.3
Well constrained by soil, land cover and geological attributes	No	No	3.4
Potential improvement of the prediction by better data	Weak	Strong	3.4
<b>Discussion</b>			
Regionalization	Easy	Difficult	4.1
Sensitivity to discharge uncertainty and signature formulation	Low	High	4.1
Discriminative power	High	Questionable	4.2
Recommend for model evaluation	Yes	Not without uncertainty quantification	4.3

966  
 967

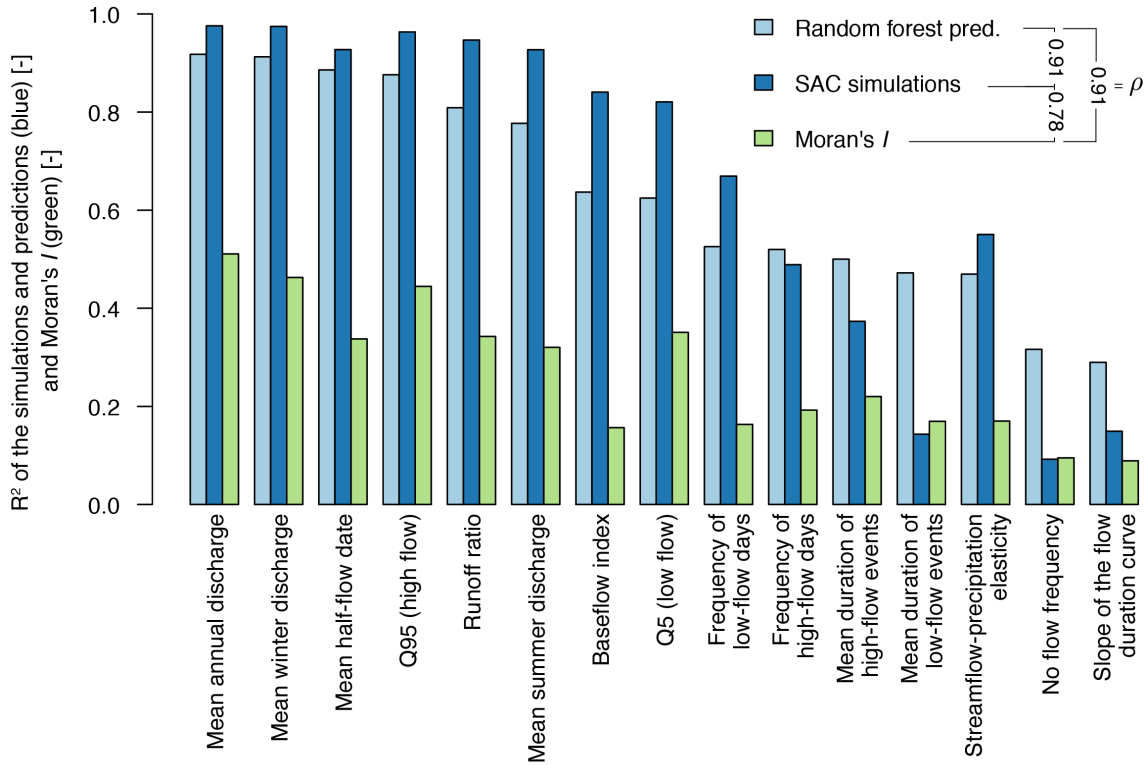
968 **Figures**  
 969



970  
 971

972 Figure 1: Comparison of the observed, predicted and simulated (first, second and third row,  
 973 respectively) mean annual discharge, baseflow index and slope of the flow duration curve (first,  
 974 second and third column, respectively). The spatial auto-correlation quantified using Moran's  $I$  is  
 975 indicated for the maps of top row. The last row combines and compares the data from the three  
 976 maps of the same column and indicates the coefficient of determination  $R^2$  for the random forest  
 977 predictions and SAC simulations computed over all the catchments.

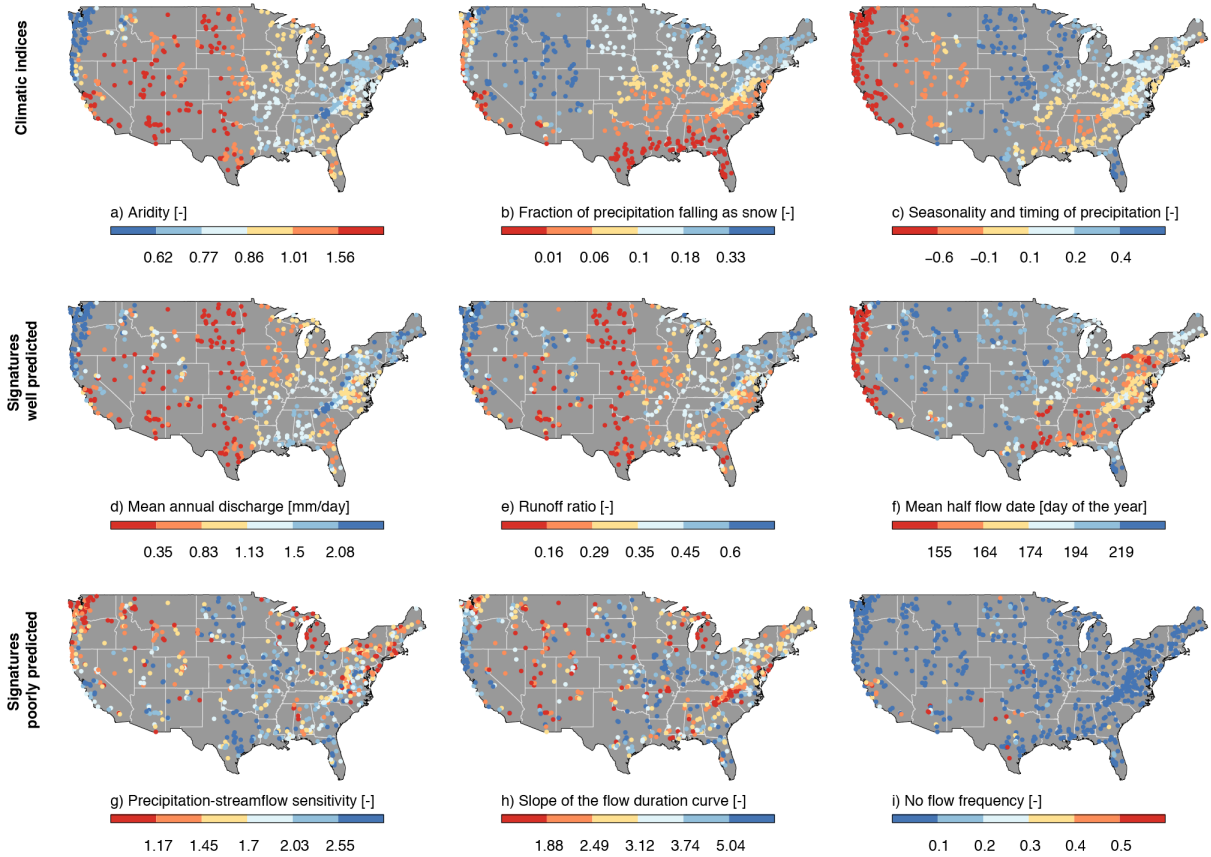
978



979

980 Figure 2: Illustration of the strong three-way relationship between how well signatures can be  
 981 predicted based on catchment attributes using a random forest ( $R^2$  between the observed and  
 982 predicted signatures, light blue), how well they can be simulated by SAC ( $R^2$  between the  
 983 observed and simulated signatures, dark blue), and the smoothness of their spatial variability over  
 984 the CONUS (Moran's  $I$ , green). The correlations between those variables are indicated in the  
 985 upper-right corner. The signatures are ordered from left to right based on how well they can be  
 986 predicted using a random forest. Each bar is based on at least 600 catchments.

987



988  
989

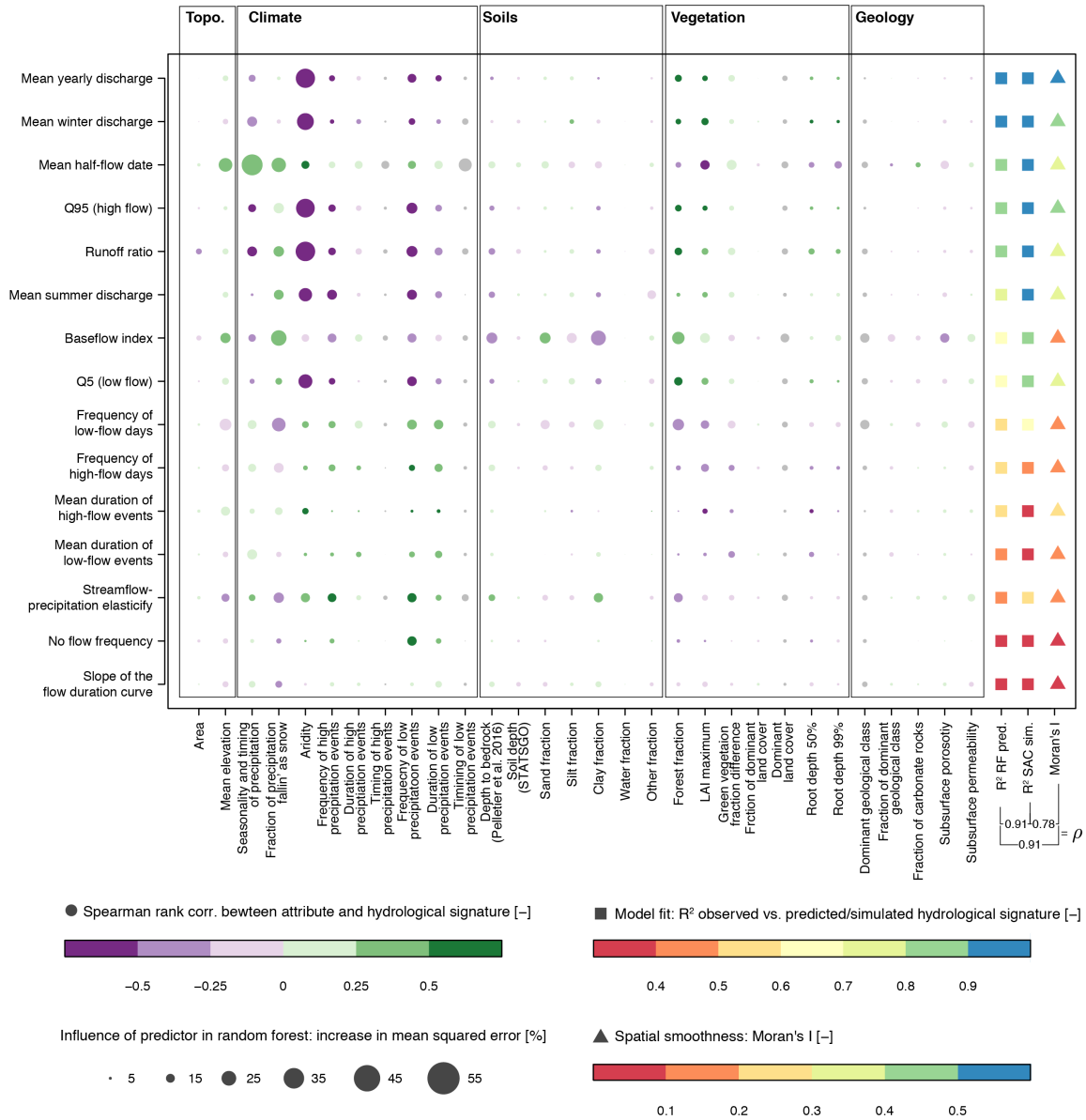
990 Figure 3: Comparison of the spatial patterns in climatic indices (top row),  
991 well-predicted hydrological signatures (middle row) and poorly-predicted hydrological signatures (bottom  
992 row). We used the same color scheme for all the maps to underscore similarities between them.  
993 Note that units and break values vary. The break values were chosen so that each color class  
994 encompasses about one sixth of the total number of catchments (except for the no flow  
995 frequency).

996

997

998

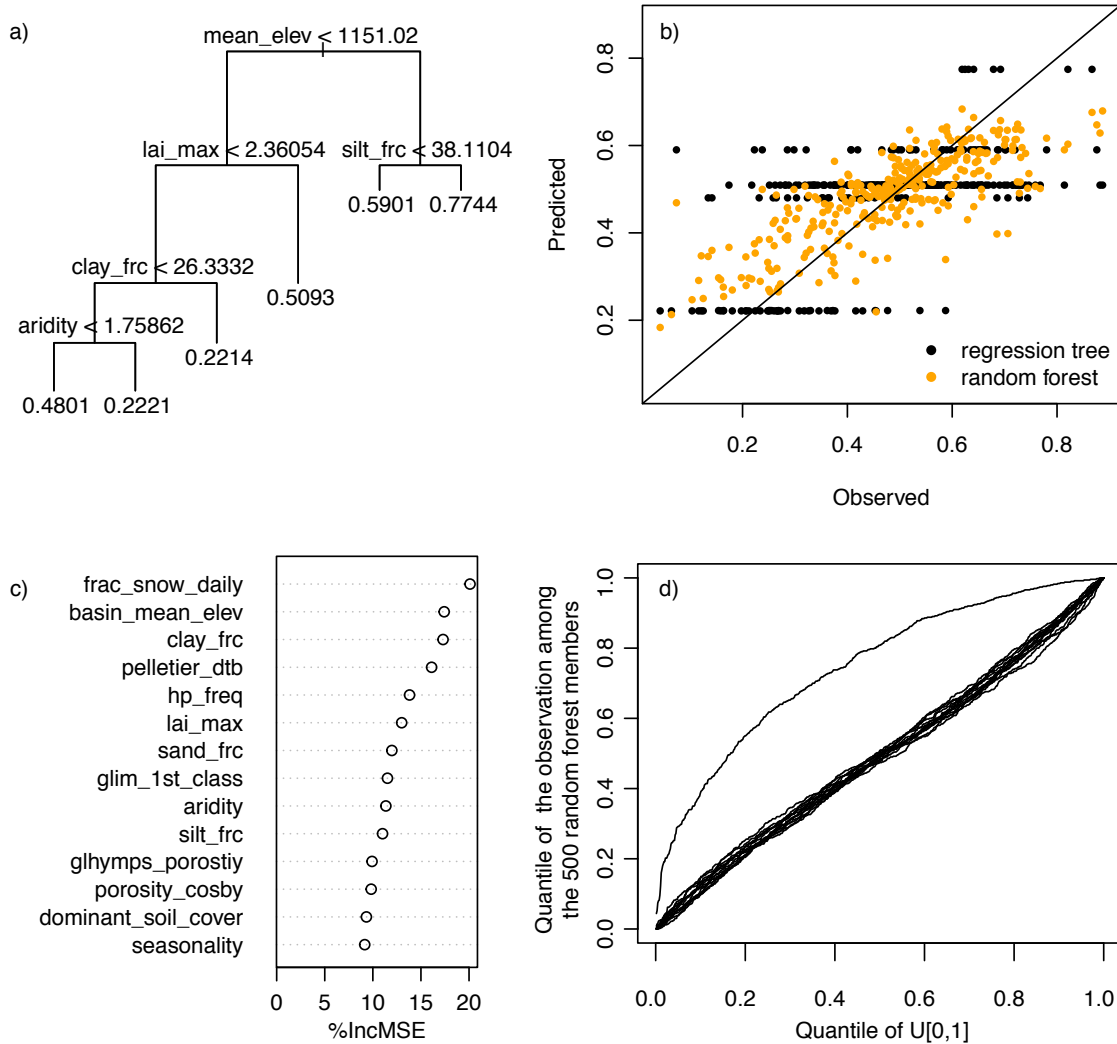
999



1000  
1001

1002 Figure 4: Signature table synthesizing the main findings of this study. Catchment attributes (x-  
1003 axis) are used to predict hydrological signatures (y-axis) using random forests. The signatures are  
1004 ordered vertically based on how well they are captured by random forests. The influence of each  
1005 catchment attribute on each signature in the random forest is measured by IncMSE and is  
1006 proportional to the size of the dots. The three right-most columns summarize the data shown in  
1007 Figure 2.

1008  
1009  
1010



1011  
1012

1013 Figure A1: a) Example of a pruned regression tree trained to predict the baseflow index. b)  
 1014 Comparison of baseflow index observations to predictions from the regression tree shown in a)  
 1015 and from a random forest, whose most influential predictors are shown in c). c) Assessment of the  
 1016 relative influence of the random forest variables for the prediction of the baseflow index, the  
 1017 predictors are ordered from the most to least influential (top to bottom). d) QQplot for the 15  
 1018 hydrological variables, lines close to the diagonal indicate reliable ensembles, the only line  
 1019 significantly departing from the diagonal is the fraction of no flow, see Laio and Tamea (2007) or  
 1020 Renard et al. (2010) for more details on how to interpret this plot.

1021